Effects of volatilization on the hydrogen isotope composition of selected *n*-alkanes

Huiling Bai [a], Lin Peng [a,*], Junji Cao [b], Xiaofeng Liu [a], Jianqiang Zhang [a], Ling Mu [a]

[a] College of Environmental Science and Engineering, Taiyuan University of Technology, Taiyuan 030024, China
[b] State Key Laboratory of Loess and Quaternary Geology, Institute of Earth Environment, Chinese Academy of Sciences, Xi'an 710075, China

ARTICLE INFO

ABSTRACT

The hydrogen isotope composition of n-C_{15} to n-C_{32} n-alkanes was measured by GC–IRMS to investigate the behavior of H isotopes during evaporation. The H isotope fractionation of n-C_{15} to n-C_{19} ranged from −8.5 to −22.5‰, demonstrating the preferential vaporization of the isotopically heavier organic compounds. The H isotope fractionation rates of n-C_{16} to n-C_{18} showed no obvious fluctuations with time (average rates were 1.1, 0.5 and 0.3‰ per day, respectively); this indicated that fractionation followed the Rayleigh model. Although less conclusive, the fractionation of H isotopes in n-C_{19} also apparently followed the Rayleigh trend. Information on fractionation rates may be useful for identifying the dominant attenuation and degradation processes for organic substances in the environment. The results also highlight potential applications of isotope fractionation factors, which were determined by regression analysis, for investigations into the behavior of organic substances in the environment.

© 2013 Elsevier B.V. All rights reserved.

1. Introduction

The *n*-alkanes, a homologous series of non-polar organic compounds, often show high concentrations in atmospheric aerosols, including total suspended particulates (TSP), particulate matter less than 10 μm (PM_{10}), $PM_{2.5}$ and PM_1 (Guo et al., 2003; Li et al., 2012; Lin, 2004; Young and Wang, 2002). Primary sources for these compounds include fossil fuel combustion and biological emissions (Bi et al., 2008; Ulevicius et al., 2010; Zhou et al., 2009); and the contributions from these two sources have been evaluated using the carbon preference index, carbon number maximum, homologue distributions, and C and H isotope variations (Ladji et al., 2009; Mansuy et al., 1997; Xie et al., 2009; Yamamoto and Kawamura, 2011). Although diagnostic parameters such as these provide important insights into the origins of organic compounds in the environment, attention still needs to be focused on how they degrade and how their concentrations are attenuated. Here we use the term "attenuation" to describe in general terms the decreases in the concentrations of the compounds brought about by evaporation and other loss processes.

Compound-specific isotope analysis (CSIA) has become a powerful analytical tool, and it has been used to investigate how physical processes (vaporization, adsorption) and chemical processes (photo-degradation, biodegradation and chemical oxidation) affect the composition of specific compounds, including the ways in which these substances are modified in the natural environment (Fischer et al., 2007; Harrington et al., 1999; Hunkeler et al., 2003; Ma et al., 2010; Oba and Naraoka, 2008). Isotope fractionation often results from the preferential evaporation of molecules containing heavier H isotopes (Kuder et al., 2009a, 2009b; Poulson and Drever, 1999); but for compounds that have hydrogen bonds, the H isotopes often show the opposite fractionation tendency (Wang and Huang, 2003). The magnitude of H isotope fractionation for short chain *n*-alkanes (n-C_7 to n-C_{14}) during evaporation has been found to range from −7.2‰ to −32.8‰ (Wang and Huang, 2001, 2003). These findings suggest that isotope signatures can be used to investigate the attenuation of the compounds'

concentrations in the environment and thus provide information on the fates of hydrocarbons in that context (Pond et al., 2002).

Isotope fractionation during evaporation is driven by the molecular forces between molecules rather than the breaking of chemical bonds within a molecule, and this phenomenon has been explained in terms of binding energies (Grootes et al., 1969) and molecular structure (Bradley, 1954). Most studies to date have focused on isotope fractionation in the context of natural attenuation, and it has become apparent that the extent of fractionation often increases over time, but there is little quantitative information on the rates at which the isotope fractionation proceeds.

In the present study, we conducted experiments to investigate the H isotope fractionation of n-alkanes; in particular, we focused on isotope fractionation rates during the evaporation process because this subject has received relatively little attention to date. The objectives of our studies were (1) to apply CSIA to investigate the behavior of organics by measuring the fractionation of H isotopes from n-alkanes and (2) to develop a diagnostic tool for studying the environmental attenuation of organic matter.

2. Experimental methods

2.1. Experimental design

All vaporization experiments were conducted in a laboratory with environmental controls. Room temperature during the experiments was 24 °C $\pm$ 1 °C, and relative humidity was 34% $\pm$ 2%. A mixed standard, composed of n-C$_{15}$ to n-C$_{32}$ dissolved in n-hexane, was used for the experiments without further purification. The purity of the test compounds ranged from 99.9% to 97.9%, and their initial concentrations were known to range from 1012 μg/ml to 1088 μg/ml. Two-milliliter brown glass vials were cleaned with dichloromethane in an ultrasonic bath for 20 min, and then the vials were wrapped with aluminum foil to avoid any potential influences of ultraviolet light on the isotope composition.

Seven pre-cleaned vials were sequentially capped with Teflon® (PTFE)-lined caps immediately after 20 μl of the standard mixture was added into them with a 25 μl microsyringe. Next, the vials were moved into a fume hood, and the caps were removed as simultaneously as possible to allow the n-alkanes to start volatilizing. The fume hood was kept running so that the evaporation process would start immediately after opening the vials. Periodically, the vials were capped and then kept in a freezer (4 °C) prior to the measurements of hydrogen isotope composition. To account for the solvent lost to evaporation, the standards were diluted again to 20 μl with n-hexane before the next aliquots were taken for hydrogen isotope analysis.

2.2. Gas chromatography (GC)

Quantification of the n-alkanes was performed with the use of a Hewlett-Packard 6890 gas chromatograph, equipped with a 30-m, fused-silica, capillary column (HP-5, 0.32 mm i.d., 0.25 μm film thickness) and a flame ionization detector. Ultra-high purity helium was used as the carrier gas, and it was delivered a constant flow rate of 1.0 ml min^{-1}. The

sample of 1 μl volume was injected in the splitless mode, and the injection port temperature was 280 °C. The temperature program for the n-alkane determinations involved three steps (1) 70 °C for 2 min, (2) heating to 290 °C at 6 °C min^{-1}, and (3) 290 °C for 30 min. The concentration of each compound during the vaporization experiments was determined by its abundance relative to the internal standard n-tetracosane-D.

2.3. Hydrogen isotope analysis

Hydrogen isotope analysis of individual n-alkanes was performed using a gas chromatography/high-temperature conversion/isotope ratio mass spectrometry (GC–TC–IRMS) system. An HP-6890 gas chromatograph, fitted with a 30 m capillary column (HP-5, 0.32 mm i.d., 0.25 μm film thickness), connected with a high-temperature pyrolysis furnace through a GC combustion-III interface to a Finnigan MAT Delta Plus-XL isotope-ratio mass spectrometer was used for these analyses. Injection was performed in the splitless mode, and the GC temperature program and the carrier gas and flow were the same as those described above for the n-alkane analyses. Individual n-alkanes separated by GC were successively pyrolyzed to H$_2$ and C at 1440 °C. The H$_2$ was then introduced into the mass spectrometer.

Recently, stable hydrogen isotope ratios (calculated as δD in per mil, ‰) have been used to investigate the sources and transport of n-alkanes (n-C$_{21}$ to n-C$_{33}$) in a polluted urban atmosphere (Yamamoto and Kawamura, 2010, 2012). Here δD values were calibrated using a reference H$_2$ gas, and they were reported relative to Vienna Standard Mean Ocean Water (VSMOW) as is the convention:

$$\delta D = \left[\left(D/^1H \right)_{sample} / \left(D/^1H \right)_{VSMOW} - 1 \right] \times 1000. \quad (1)$$

The standard deviation for the δD analysis of each compound was <6‰.

For the correction of D/^{1}H, the H$_3$ factor was determined daily prior to sample analysis by measuring the (mass-3) / (mass-2)((HD$^+$ + H$_3^+$) / H$_2^+$) ion current ratio of a sample over a range of H$_2$ pressures in the ion source. Least-squares regression was then used to find the value of the H$_3$ factor. The mass spectrometer was tuned to ensure that the H$_3$ factor was always ~8 and the daily variability <0.1. A set of laboratory standards (n-C$_{12}$, n-C$_{14}$, n-C$_{16}$, n-C$_{18}$, n-C$_{20}$, n-C$_{22}$, n-C$_{25}$, n-C$_{28}$, n-C$_{30}$ and n-C$_{32}$) with known δD values was injected after every sixth sample analysis to test the stability of the instrument. The fluctuation of δD values for the standard n-alkanes was smaller than 4‰. The δD values reported for the samples were the average of three repeat analyses.

3. Results and discussion

3.1. Hydrogen isotope fractionation during evaporation

The residual n-C$_{15}$ to n-C$_{19}$ n-alkanes in the test solutions became depleted in D as a result of evaporation; that is, when 2.4, 0.8, 7.1, 36.5 and 50.6% of initial n-C$_{15}$ to n-C$_{19}$ n-alkanes remained, the D depletions were −15.1‰ for n-C$_{15}$, −22.5‰ for n-C$_{16}$, −16.0‰ for n-C$_{17}$, −10.2‰ for n-C$_{18}$ and −8.0‰ for n-C$_{19}$ (Table 1). Larger variations in concentrations clearly

Table 1
Hydrogen isotope composition of residual n-C_{15}–n-C_{19} alkanes as a function of evaporation time.

n-Alkane	Time (d)	F	$\delta D \pm$ S.D. (‰)	δD_{F-I}
C_{15}	0	1	-101.2 ± 1.6	
	5	0.228	-111.1 ± 4.5	-10.0
	8	0.024	-116.3 ± 5.6	-15.1
C_{16}	0	1	-72.1 ± 1.8	
	5	0.710	-77.7 ± 1.5	-5.7
	8	0.343	-80.2 ± 2.1	-8.2
	12	0.159	-85.1 ± 5.0	-13.0
	17	0.046	-89.7 ± 3.6	-17.6
	23	0.008	-94.6 ± 4.8	-22.5
C_{17}	0	1	-171.2 ± 0.7	
	5	0.985	-173.4 ± 3.8	-2.2
	8	0.657	-175.9 ± 1.3	-4.6
	12	0.576	-177.8 ± 2.5	-6.5
	17	0.438	-180.3 ± 5.6	-9.1
	23	0.295	-184.4 ± 3.3	-13.2
	30	0.195	-187.2 ± 0.1	-16.0
	38	0.071	-187.2 ± 3.2	-16.0
C_{18}	0	1	-62.7 ± 1.6	
	5	0.953	-64.1 ± 0.2	-1.5
	8	0.764	-63.9 ± 1.6	-1.3
	12	0.751	-65.4 ± 1.0	-2.7
	17	0.695	-67.3 ± 2.4	-4.6
	23	0.596	-68.6 ± 1.3	-5.9
	30	0.596	-71.3 ± 0.8	-8.7
	38	0.365	-72.8 ± 1.1	-10.2
C_{19}	0	1	-256.5 ± 1.7	
	5	0.961	-260.3 ± 1.3	-3.8
	8	0.795	-260.7 ± 1.1	-4.2
	12	0.799	-262.8 ± 2.0	-6.3
	17	0.715	-263.9 ± 2.9	-7.4
	23	0.682	-263.3 ± 0.9	-6.8
	30	0.667	-265.1 ± 0.7	-8.5
	38	0.506	-264.5 ± 0.9	-8.0

F and δD are as defined in Fig. 1. δD_{F-I} is the difference between the δD at a given time and under the initial conditions. S.D. stands for standard deviation.

corresponded with greater isotopic fractionation, and so under the same experimental conditions, the shorter chain n-alkanes always were more depleted D than the longer-chain homologues. The negative values for δD_{F-I} ($=\delta D_{Final} - \delta D_{Initial}$) show that organic molecules containing heavier isotopes volatilized preferentially which is in contrast to the normal isotope fractionation pattern associated with the aqueous-phase attenuation or biodegradation of organic compounds (where there is enrichment of the heavy isotopes in residual materials) (Kuder et al., 2009a, 2009b). In other words, the evaporation of n-alkanes induced an inverse H isotope effect (IE) in our experimental conditions (Braeckevelt et al., 2012), and this result is consistent with the findings reported by Wang and Huang (2003). The larger isotopic fractionation of the short chain n-alkanes raises the potential for estimating the amount of attenuation that has occurred. In particular, the relationships between isotope variations and the corresponding fractions of residuals for strong IEs have been inferred (Mariotti et al., 1981; Rayleigh, 1902).

Inverse C and H IE phenomena (Braeckevelt et al., 2012; Kuder et al., 2009a, 2009b) have been explained by the higher vapor pressures of the isotopically heavier species in the non-aqueous phase compared with the ones of lighter isotopes (Grootes et al., 1969); note however that this explanation is not applicable to the IE for Cl (Poulson and Drever, 1999). These higher vapor pressures, in turn, have been attributed to the smaller intermolecular binding energies of the heavier isotopes; that is, smaller intermolecular binding energies induce the preferential volatilization of molecules bearing the heavier isotopes.

At the conditions used in our studies, ~90% of the longer chain n-alkanes (n-C_{20} to n-C_{32}) remained in the test solutions (Table 2), and the H isotope fractionations of these organics ranged from -1.2‰ to -5.6‰ (Table 3). These values are well within normal analytical uncertainty (6‰) of the hydrogen isotope ratio analysis. Nonetheless, the n-alkane concentrations and their isotopic compositions all gradually decreased over the time course of the study (Fig. 1), and the level of reduction was moderate relative to the ones of n-C_{15} to n-C_{19} homologues. That is, a smaller decrease in concentration corresponded with a lower level of isotopic fractionation; this is consistent with the pattern observed during bioremediation of petroleum contaminants (Pond et al., 2002).

Furthermore, it is possible that the H IE for n-C_{20} to n-C_{32} would have been more conspicuous if the incubation temperature were higher. That is, the overall extent of isotope fractionation depends not only on the compounds and particular isotope(s) of interest but also on the evaporation conditions (Kuder et al., 2009a, 2009b). Indeed, the results of all the studies of n-alkanes indicate that isotopic fractionation is strongly dependent on experimental residual concentrations. In this regard, the apparent lack of H isotope effects for n-C_{20} to n-C_{32} can be regarded as evidence that the H isotopic composition of specific n-alkanes may be useful for evaluating the contributions of fossil fuel and higher plant sources for atmospheric samples (Yamamoto and Kawamura, 2010, 2012). Given the effects of temperature on the C isotopic fractionation (Poulson and Drever, 1999), there should also require a further research on the relationship between the temperatures and H isotopic fractionation for the accurate application in the environmental analysis when the evaporation was the dominant attenuation process.

The δD_{F-I} values were comparatively small during the initial stages of our experiment, with values of -10.0, -5.7, -2.2, -1.5 and -3.8‰ for the n-C_{15} to n-C_{19} compounds, respectively (Table 1). As the evaporation experiments proceeded and the residual concentrations decreased, the

Table 2
Residual concentrations (mg/ml) of n-C_{20} to n-C_{32} n-alkanes during volatilization.

n-alkane	Time in days							
	0	5	8	12	17	23	30	38
C_{20}	1.087	1.073	1.060	1.044	1.036	1.012	1.008	1.007
C_{21}	1.078	1.065	1.036	1.029	1.030	1.029	1.017	1.003
C_{22}	1.051	1.036	1.033	1.028	1.011	1.006	0.999	0.996
C_{23}	1.041	1.034	1.026	1.021	1.016	1.008	0.999	0.991
C_{24}	1.028	1.022	1.012	1.007	1.000	0.992	0.980	0.976
C_{25}	1.016	1.014	1.009	0.999	0.978	0.973	0.966	0.988
C_{26}	1.018	1.015	1.008	1.000	0.994	0.989	0.975	0.983
C_{27}	1.012	1.007	0.998	0.971	0.985	0.980	0.992	0.974
C_{28}	1.015	1.006	0.992	0.985	1.002	0.982	0.979	0.971
C_{29}	1.059	1.053	1.028	1.048	1.033	1.028	1.027	1.023
C_{30}	1.030	1.026	1.014	1.006	1.001	0.996	0.993	0.993
C_{31}	1.048	1.039	1.035	1.027	1.022	1.020	1.017	1.015
C_{32}	1.085	1.077	1.074	1.069	1.063	1.058	1.055	1.055

Table 3
Hydrogen isotope composition (δD in ‰) of residual n-C_{20} to n-C_{32} n-alkanes during evaporation.

n-Alkane	Time in days								$\delta D_{F\text{-}I}$(‰)
	0	5	8	12	17	23	30	38	
C_{20}	-57.4 ± 2.7[a]	-57.9 ± 0.2	-59.8 ± 2.1	-59.3 ± 2.0	-61.4 ± 2.6	-60.9 ± 2.7	-59.6 ± 1.2	-63.0 ± 3.8	-5.6
C_{21}	-174.1 ± 1.5	-178.0 ± 0.2	-176.2 ± 1.9	-177.3 ± 1.5	-177.5 ± 1.6	-178.8 ± 1.9	-179.7 ± 0.9	-179.7 ± 0.9	-5.6
C_{22}	-63.0 ± 4.2	-63.4 ± 1.1	-63.6 ± 1.9	-64.4 ± 2.0	-66.8 ± 2.3	-65.3 ± 1.8	-66.4 ± 1.3	-66.9 ± 2.6	-3.9
C_{23}	-62.1 ± 2.5	-63.2 ± 0.3	-64.0 ± 2.3	-62.9 ± 2.1	-64.7 ± 1.6	-66.3 ± 1.1	-65.4 ± 1.5	-66.2 ± 2.7	-4.1
C_{24}	-28.5 ± 4.2	-28.6 ± 1.0	-28.0 ± 0.6	-28.5 ± 3.6	-30.6 ± 1.8	-30.4 ± 2.0	-31.4 ± 1.2	-33.2 ± 3.6	-4.7
C_{25}	-119.7 ± 2.4	-120.2 ± 2.6	-120.5 ± 1.4	-120.3 ± 2.6	-122.1 ± 1.2	-122.6 ± 0.4	-122.9 ± 0.6	-124.0 ± 0.8	-4.3
C_{26}	-45.3 ± 0.9	-45.8 ± 1.8	-45.5 ± 1.1	-46.5 ± 2.1	-46.1 ± 1.3	-47.6 ± 0.2	-47.3 ± 0.9	-49.2 ± 3.0	-3.9
C_{27}	-169.0 ± 0.7	-170.8 ± 1.2	-170.5 ± 0.8	-170.2 ± 2.4	-171.2 ± 2.5	-171.4 ± 0.7	-171.7 ± 1.2	-172.6 ± 0.9	-3.6
C_{28}	-264.6 ± 3.4	-267.8 ± 0.5	-268.1 ± 0.3	-268.5 ± 2.2	-269.3 ± 2.0	-269.5 ± 0.7	-269.3 ± 1.3	-269.6 ± 0.4	-5.0
C_{29}	-175.9 ± 0.8	-174.8 ± 0.4	-176.6 ± 0.9	-176.9 ± 1.6	-177.6 ± 0.8	-178.1 ± 1.2	-178.6 ± 0.5	-178.0 ± 1.0	-2.2
C_{30}	-31.5 ± 1.3	-31.8 ± 2.5	-31.4 ± 0.9	-29.6 ± 0.5	-31.6 ± 1.3	-31.9 ± 2.2	-31.8 ± 0.6	-32.7 ± 1.5	-1.2
C_{31}	-172.5 ± 1.8	-173.7 ± 2.5	-173.7 ± 0.5	-174.0 ± 0.9	-175.3 ± 1.1	-175.2 ± 1.8	-175.6 ± 1.1	-174.5 ± 0.1	-2.1
C_{32}	-223.5 ± 2.1	-224.3 ± 1.3	-224.5 ± 0.4	-224.5 ± 1.2	-225.0 ± 1.5	-225.4 ± 0.7	-225.7 ± 0.6	-225.7 ± 1.8	-2.2

[a] Arithmetic mean $\pm$ standard deviation.

magnitude of the isotope fractionation increased. This phenomenon may be explained by the notion that the pool of n-alkanes initially is large enough to buffer the variations in isotope composition, but this buffering effect gradually diminishes as the residual pool decreases (Pond et al., 2002). A comparison of the data for the n-alkane homologues shows that the isotope fractionation generally increases with the

evaporation time, for example, n-C_{19} had the maximum fractionation of -8.5‰ occurred from day 30 on, and -7.4‰ of this occurred from day 17 on. n-C_{17} had a fractionation of -16.0‰ from day 38 on, and -13.2‰ of this occurred from day 23 on.

We note that measurements of δD for the products were beyond the scope of our study, but the integrated δD of the
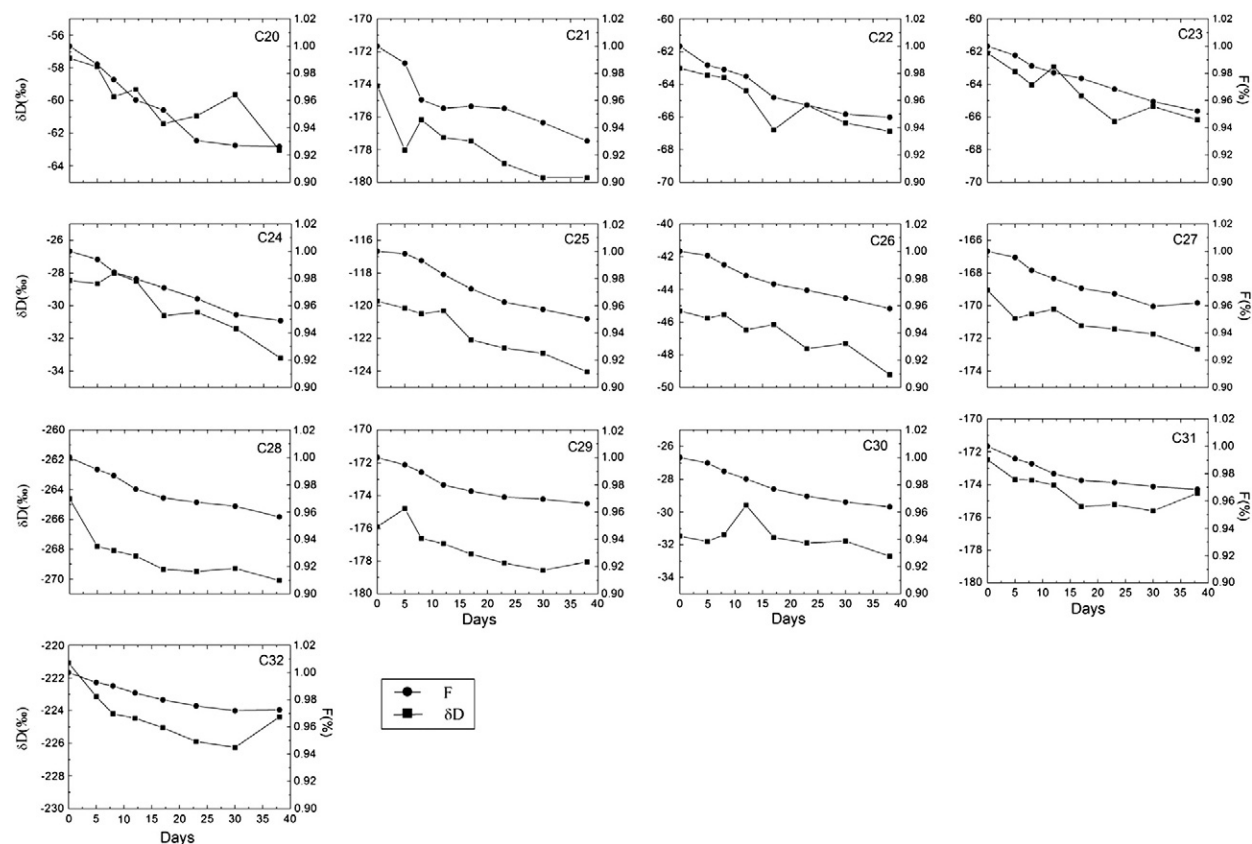
Fig. 1. Hydrogen isotope composition (δD) and remaining fractions (F) of n-C_{20}–n-C_{32} alkanes versus time during volatilization. δD is the hydrogen isotope ratio of the residual reported in the conventional delta (δ) notation relative to Vienna standard mean ocean water (see Eq. (1)). F (unitless) is the ratio of an n-alkane's concentration at specific evaporation time compared with its initial concentration.

gas-phase products after complete evaporation of the test substances should have matched their initial δD (Hunkeler et al., 2001). In other words, the isotopic ratio should have been conserved. This means that the isotope composition of each gas phase n-alkane should be the most positive at the beginning of the experiment and become increasingly more negative until the initial isotope composition of liquid phase is reached, assuming none of the compounds are destroyed or lost by some other means. This contention could be and should be tested by comparing the isotope compositions of the initial reactants, the residual reactants, and the gas-phase products.

3.2. Features of hydrogen isotope fractionation during evaporation

Isotope fractionation can be very different in closed versus open systems. A Rayleigh process occurs in an open system when one phase is removed continually and the equilibrium that would occur in a close system does not develop. In the experiments we conducted, the removal of the vapor produced from the liquid phase in the vials began immediately, and so the course of vaporization should approximate a Rayleigh process. Thus

$$\delta D = (\delta D_i + 1000)F^{(\alpha-1)} - 1000. \tag{2}$$

Here, δD_i denotes the hydrogen isotope ratios for each of the n-alkanes in the initial solution, δD stands for the ratios

when a specific fraction (F) of the reactants remained, and α is the fractionation factor. Rearrangement of Eq. (2) yields:

$$\ln((\delta D + 1000)/(\delta D_i + 1000)) = (\alpha - 1)\ln F. \tag{3}$$

If evaporation follows the Rayleigh model, a plot of ln$[(\delta D + 1000) / (\delta D_i + 1000)]$ vs. ln$F$ should result in a straight line with a slope of $(\alpha - 1)$, and linearity would indicate that the fractionation factor remained constant during the experiment.

Regression analyses of this type were run for n-C_{16} to n-C_{19} but not for n-C_{15} because the data for that homologue were insufficient for that type of analysis (Fig. 2). Significant linear least-squares fits between ln$[(\delta D + 1000) / (\delta D_i + 1000)]$ and ln$F$ were found for n-C_{16}, n-C_{17} and n-C_{18} (R^2 values were 0.975, 0.815 and 0.779, respectively), and this suggests that the hydrogen isotope fractionation due to evaporation followed the Rayleigh model. The lower R^2 of 0.567 for n-C_{19} indicates that the fractionation of H isotopes from that compound did not follow the Rayleigh fractionation as closely; this could be a result of the volatilization conditions as well as the difference in extent of fractionation. That is, the relatively high fraction of residual n-C_{19} and the low isotopic variation, which were 50.6% and −8.0‰ respectively, may have masked the inherent isotopic fractionation tendency over the time course considered. Further evaporation studies may be needed to reveal the real fractionation trends for this compound.

The isotope fractionation factor (α) represents the relative difference in isotope composition between the two substances
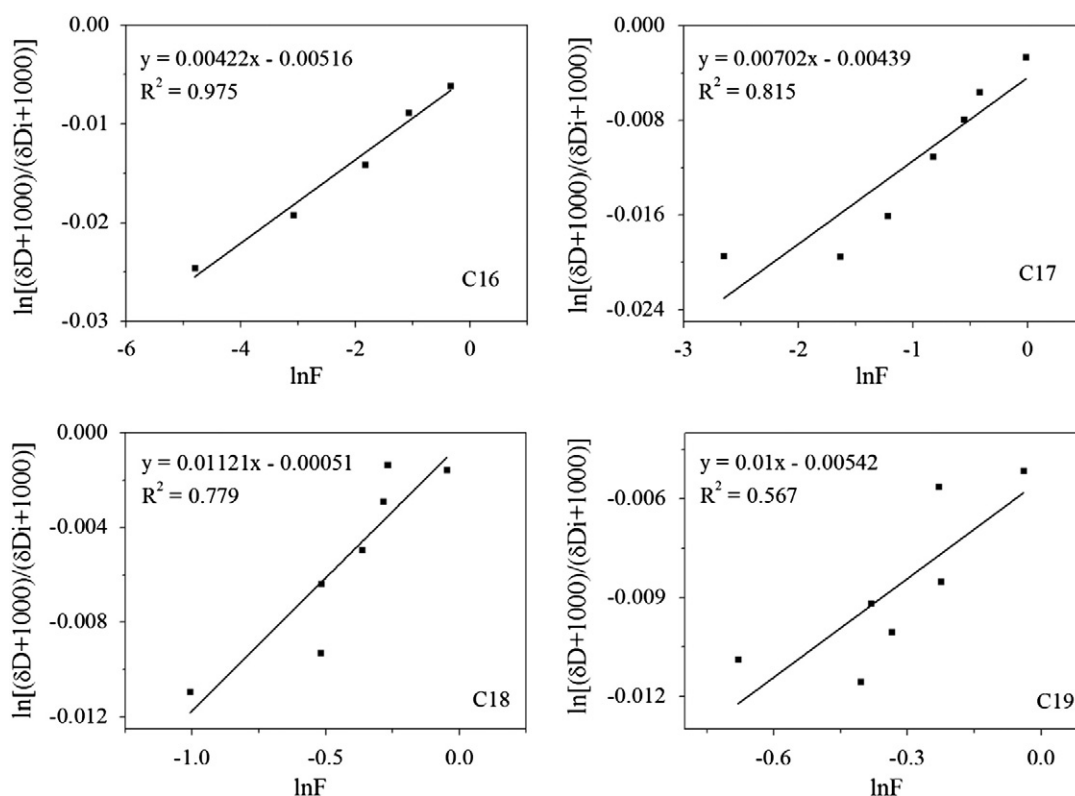

Fig. 2. Relationships between ln$[(\delta D + 1000) / (\delta D_i + 1000)]$ and ln$F$ for n-C_{16}–n-C_{19} during evaporation. The subscript i denotes the initial normalized ratio.

(Heraty et al., 1999). Here the two substances of interest were (1) the initial mixed n-alkanes and (2) their liquid residues in the evaporation studies. Note that α has also been used in reference to the ratios of specific reaction rates between the heavy and light isotopes (Elsner et al., 2005). The slopes of the $\ln[(\delta D + 1000) / (\delta D_i + 1000)]$ versus $\ln F$ regressions give fractionation factors for the n-C_{16} to n-C_{19} n-alkanes of 1.0042, 1.0070, 1.0112 and 1.0100, respectively. As the fractionation factors were all greater than unity, one would predict that the gas-phase products would be enriched in heavy isotopes because the volatilization rates of molecules bearing the heavier isotope were faster than the ones of molecules containing the lighter isotope, but as noted above those measurements were beyond the scope of this study.

More generally, fractionation factors for evaporation can be considered indicative of the phase-distribution of semi-volatile organic compounds. The corresponding enrichment factors (ε), equal to $(\alpha - 1) \times 1000$, were 4.2, 7.0, 11.2 and 10.0‰ for n-C_{16} to n-C_{19}, respectively, meaning that the isotope ratios of the formed products were always isotopically heavier (by a factor ε) than the ratios of the substrates for the specific residual fraction during the evaporation study. It is obvious that the enrichment factors increased with n-alkane chain length, and this supports a conclusion drawn from previous research (Wang and Huang, 2003). It is worth noting that the magnitudes of the enrichment factors in the Wang and Huang (2003) study differed from ours. These differences may have been caused by the larger evaporation extent (F values) for C_{16} and C_{17} n-alkanes and the weaker regression analyses for n-C_{18} and n-C_{19} in our experiment than that in the research of Wang and Huang (2003).

In addition to the determination of α, the value of F, that is, the ratio of the n-alkane's concentration at specific evaporation time (shown as the subscript t) compared with its initial concentration, denoted by the subscript i, is a matter interest in this field of research. For n-alkanes, F is thus defined as follows:

$$F = [n - \text{alkanes}]_t / [n - \text{alkanes}]_i \quad (4)$$

where the brackets denote concentrations. Solving Eq. (2) for F yields:

$$F = [(\delta D + 1000)/(\delta D_i + 1000)]^{1/(\alpha-1)}. \quad (5)$$

If one assumes that the variation in the concentrations is due only to a reaction with a fixed value of α, Eq. (5) allows us to calculate expected concentration ratios based on the observed isotopic signatures. Using this ratio, the extent of degradation (B) can be estimated as follows (Meckenstock et al., 1999; Richnow et al., 1999):

$$B(\%) = (1 - F) \times 100. \quad (6)$$

Eqs. (5) and (6) show that when the isotopic ratios of the reactants and the residues are both known, fractionation factors can be used to estimate the extent to which the concentrations of specific n-alkanes have been attenuated: this concept has been verified in previous studies of biodegradation (Gray et al., 2002; Mancini et al., 2002). Even though the

conditions under which evaporation occurs in the natural environment and laboratory studies can be extremely different, fractionation factors should remain constant because of the fixed relationship between the concentrations and isotopic composition (namely the Rayleigh model). Therefore, at least in theory, empirically-determined fractionation factors could be used to calculate the volatility and extent of volatilization of n-alkanes under ambient environmental conditions. Our study thus highlights the value of the information on H isotope fractionation in this environmental context, and further research on isotope fractionation factors for various organic substances should provide additional insights into the phase distribution and environmental attenuation of these compounds.

3.3. Average rate of hydrogen isotope fractionation

The sign of δD_{F-I} indicates whether enrichment or depletion of the hydrogen isotopes has occurred, and its magnitude reflects the variations in the isotopic composition during the study period. Therefore, plots of the absolute values of δD_{F-I} versus time can be used to compare the extent of isotope fractionation for volatilization, photo- and bio-degradation processes. The relationships between the absolute values of δD_{F-I} for n-C_{16} to n-C_{19} and evaporation times are plotted in Fig. 3. It is apparent that the absolute values of δD_{F-I} increased with time for these n-alkanes. Also evident in the plot is the fact that the extent of isotope fractionation decreased with carbon chain length. These findings provide the basis for a comparative approach that can be used to evaluate the resistance of organic substances to degradation and to determine the primary degradation process for specific compounds.

Isotope fractionation rates provide further information on the dominant processes responsible for the attenuation of organic compounds and also reveal the fundamentals of the fractionation process. Our data suggest that the hydrogen isotope fractionation rates were constant throughout the evaporation study. Therefore, the average fractionation rate can be expressed as follows:
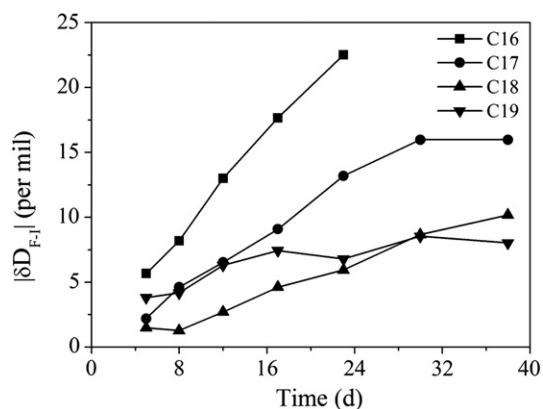
$$HFR = |\delta D_{F-I}|/T \quad (7)$$

Fig. 3. The absolute values of hydrogen isotope fractionation of n-C_{16}–n-C_{19} n-alkanes as a function of evaporation time.

where HFR is the average hydrogen isotope fractionation rate expressed in ‰ per day, and T is the evaporation time with the unit of day. The average HFR values for n-C_{16} to n-C_{19} are plotted in Fig. 4, and even though the calculated HFR's were smaller than the standard deviations, there are still significant implications for these results. That is, there were no obvious fluctuations in the fractionation rates except for n-C_{19}, and for that homologue, the fluctuation in the rate was up to 0.6‰. In other words, the fractionation rates for n-C_{16} to n-C_{18} were as essentially constant throughout the evaporation study, with HFR values of 1.1, 0.5 and 0.3‰ per day respectively. The small variations in the fractionation rates over time are consistent with the significant correlations between $\ln[(\delta D + 1000) / (\delta D_i + 1000)]$ and $\ln F$ for n-C_{16} to n-C_{18}; that is, both sets of results support the conclusion that the H isotope fractionation rates were stable over time.

3.4. Applications of isotope fractionation to field studies

Studies of isotope composition have become of increasing interest to environmental scientists because CSIA can provide independent constraints useful for evaluating the origins of chemicals in the environment. For example, O'Malley et al. (1994) suggested that carbon isotopic ratios could be applied to source apportionment studies for polycyclic aromatic hydrocarbons (PAHs). That suggestion was based on the observation that carbon isotope ratios of PAHs isolated from environmental samples were maintained after vaporization, photo- and bio-degradation, and this forms the theoretical basis for PAH source apportionments based on carbon isotopes. Similarly, research on the relationships between weathered crude oil and suspected sources have been undertaken using the carbon isotopic composition of n-alkanes (Mansuy et al., 1997); the authors of that study and others (Pond et al., 2002; Sun et al., 2005) have argued persuasively that information on hydrogen and carbon isotopes can be useful markers for source apportionments of petroleum hydrocarbons. On the other hand, the comparatively stable isotopic composition of some specific organics relative to degradation or attenuation processes may make these compounds more useful for tracing primary emission sources.
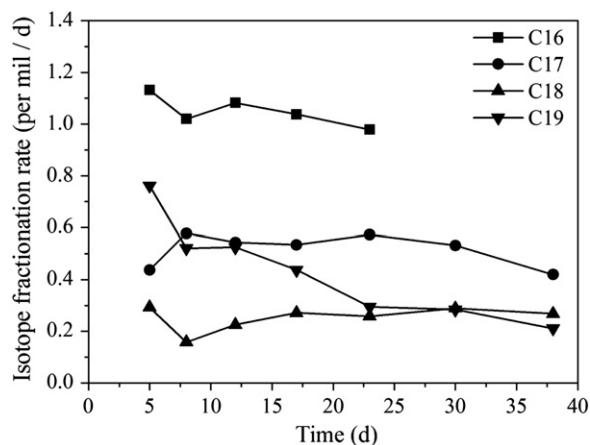

Fig. 4. Hydrogen isotope fractionation rates of n-C_{16} to n-C_{19} n-alkanes during the evaporation process.

H isotopic fractionation effects can provide unique insights into the behavior of various organic compounds because the H isotopes typically exhibit far greater fractionation than the C isotopes. Moreover, the behavior of isotopes in organic compounds can shed light on the transformation processes through consideration of isotope fractionation factors and fractionation rates. Indeed, this concept has been extended to include studies of the bioremediation of petroleum contamination by measuring the H isotope ratios of n-alkanes (Pond et al., 2002). Unfortunately, environmental processes other than evaporation, including adsorption, photo-degradation and biodegradation, also can induce H isotope fractionation and in so doing confound the interpretation of H isotope data from field studies.

In this regard, the isotope fractionation factors obtained from laboratory experiments could be used to evaluate the attenuation of individual organic compounds in situ (Richnow et al., 2003). Taking volatilization as an example, soil vapor extraction and air sparging may be responsible for much of the removal of organics in the subsurface, and these processes could cause potentially significant isotope fractionation. In that case, fractionation factors can provide useful qualitative and possible quantitative information as to the remediation efficiency. In view of the potential field applications in the atmospheric environment, the H isotope fractionation factor could serve as an auxiliary tool for distinguishing evaporation from other transformation (sorption, photo- and biodegradation) processes for semi-volatile organic compounds. These processes are important because they act on atmospheric PM both during production and transport. The application of this tool is based on the fact that sorption does not cause significant H isotope fractionation while both photo- and bio-degradation induce the opposite H isotopic fractionation effect compared with evaporation (Fischer et al., 2008; Harrington et al., 1999; Oba and Naraoka, 2007). In this way, fractionation factors may provide qualitative information on the relative contributions of particulate and gas-phase sources to semi-volatile organic compounds found in the atmosphere. Fractionation rates could be used as fingerprints of degradation pathways for organic matter when a single attenuation process is the primary means by which specific organic compounds are removed from the atmosphere.

Of course, multiple degradation processes normally occur simultaneously, and these may pose difficulties for the interpretation of isotope fractionation in field studies. Nevertheless, isotope fractionation factors for two or more elements in specific compounds, a multi-dimensional isotope analysis, may enable researchers to unravel the competing effects. For example, two-dimensional isotope fractionation (2D-CSIA) procedure involving both C and H isotopic compositions was used by Zwank et al. (2005) to determine whether the observed fractionation of the two isotopic elements was governed by a single process or multiple ones. Fischer et al. (2007) compared the biodegradation of benzene under anoxic versus oxic conditions through the use of 2D carbon- and hydrogen-CSIA. The 2D approach also has been used to separate the IEs of volatilization from those of biodegradation for methyl tertiary butyl ether (Kuder et al., 2005). Some studies have used 2D-CSIA to investigate IEs during evaporation. For example, a negative correlation between $\delta^{13}C$ and $\delta^{37}Cl$ of chlorinated aliphatic hydrocarbons has been observed,

and this relationship theoretically could be used to distinguish evaporation from biodegradation in contaminated systems (Huang et al., 1999; Jeannottat and Hunkeler, 2012).

4. Conclusions

Measurements of H isotopes by GC–TC–IRMS showed that the fractionation of stable hydrogen isotopes from a subset of n-alkanes during evaporation is consistent with the Rayleigh model. That is, the H isotope fractionation for n-C_{15} to n-C_{19} n-alkanes during evaporation ranged from $-8.5‰$ to $-22.5‰$, while those for n-C_{20} to n-C_{32} were ranging from $-1.2‰$ to $-5.6‰$. Furthermore, the hydrogen isotope fractionation rates for n-C_{16} to n-C_{18} were nearly stable over the course of the evaporation study, with observed HFR values of 1.1, 0.5 and 0.3‰ per day respectively; in comparison, the fluctuations in HFR for n-C_{19} were larger, up to 0.6‰.

The information on H isotope fractionation of the lower molecule-weight homologues (n-C_{15}–n-C_{19}) investigated in our study is useful not only for understanding the behavior of the H isotopes but also for evaluating the attenuation of organic compound concentrations in the environment. On the other hand, the nearly unaltered isotope composition of longer chain n-alkanes (n-C_{20}–n-C_{32}) we observed indicates that these homologues are better suited as tracers for the relevant emission sources when the environmental temperature is ~24 °C and volatilization is the primary attenuation process. Strong correlations between $\ln[(\delta D + 1000) / (\delta D_i + 1000)]$ and $\ln F$ for n-C_{16} to n-C_{18} showed that the H isotope fractionation rates were stable throughout the study. As more information becomes available on the behavior of isotopes during photo- and bio-degradation, it eventually may be possible to model the attenuation pathways for specific organic compounds.

Along these lines, the establishment of data base for isotope fractionation factors and rates would facilitate investigations into the extent and relative importance of specific degradation processes for environmental organic matter in field studies. Moreover, the 2D-CSIA approach, in combination with information on isotope kinetics, may shed additional light on the degradation and attenuation processes. Finally, further research on the isotope fractionation rates of organic compounds under natural conditions is needed for comparison with laboratory investigations; such measurements will provide for a more comprehensive understanding the behavior of organic compounds in the environment.

Acknowledgments

References

Bi, X.H., Simoneit, B.R.T., Sheng, G.Y., Ma, S.X., Fu, J.M., 2008. Composition and major sources of organic compounds in urban aerosols. Atmos. Res. 88, 256–265.

Bradley, D.C., 1954. Fractionation of isotopes by distillation of some organic substances. Nature 173, 260–261.

Braeckevelt, M., Fischer, A., Kastner, M., 2012. Field applicability of compound-specific isotope analysis (CSIA) for characterization and quantification of in situ contaminant degradation in aquifers. Appl. Microbiol. Biotechnol. 94, 1401–1421.

Elsner, M., Zwank, L., Hunkeler, D., Schwarzenbach, R.P., 2005. A new concept linking observable stable isotope fractionation to transformation pathways of organic pollutants. Environ. Sci. Technol. 39, 6896–6916.

Fischer, A., Theuerkorn, k, Stelzer, N., Gehre, M., Thullner, M., Richnow, H.H., 2007. Applicability of stable isotope fractionation analysis for the characterization of benzene biodegradation in a BTEX-contaminated aquifer. Environ. Sci. Technol. 41, 3689–3696.

Fischer, A., Herklotz, I., Herrmann, S., Thullner, M., Weelink, S.A.B., Stams, A.J.M., Schlömann, M., Richnow, H.-H., Vogt, C., 2008. Combined carbon and hydrogen isotope fractionation investigations for elucidating Benzene biodegradation pathways. Environ. Sci. Technol. 42, 4356–4363.

Gray, J.R., Lacrampe-Couloume, G., Gandhi, D., Scow, K.M., Wilson, R.D., Mackay, D.M., Lollar, B.S., 2002. Carbon and hydrogen isotopic fractionation during biodegradation of methyl tert-butyl ether. Environ. Sci. Technol. 36, 1931–1938.

Grootes, P.M., Mook, W.G., Vogel, J.C., 1969. Isotopic fractionation between gaseous and condensed carbon dioxide. Z. Phys. 221, 257–273.

Guo, Z.G., Sheng, L.F., Feng, J.L., Fang, M., 2003. Seasonal variation of solvent extractable organic compounds in the aerosols in Qingdao, China. Atmos. Environ. 37, 1825–1834.

Harrington, R.R., Poulson, S.R., Drever, J.I., Colberg, P.J.S., Kelly, E.F., 1999. Carbon isotope systematics of monoaromatic hydrocarbons vaporization and adsorption experiments. Org. Geochem. 30, 765–775.

Heraty, L.J., Fuller, M.E., Huang Jr., L., Sturchio, T.A., N.C., 1999. Isotope fractionation of hydrogen and chlorine by microbial degradation of dichloromethane. Org. Geochem. 30, 793–799.

Huang, L., Sturchio, N.C., Abrajano, T.J., Heraty, L.J., Holt, B.D., 1999. Carbon and chlorine isotope fractionation of chlorinated aliphatic hydrocarbons by evaporation. Org. Geochem. 30, 777–785.

Hunkeler, D., Andersen, N., Aravena, R., Bernasconi, S.M., Butler, B.J., 2001. Hydrogen and carbon isotope fractionation during aerobic biodegradation of benzene. Environ. Sci. Technol. 35, 3462–3467.

Hunkeler, D., Aravena, R., Parker, B.L., Cherry, J.A., Diao, X., 2003. Monitoring oxidation of chlorinated ethenes by permanganate in groundwater using stable isotopes laboratory and field studies. Environ. Sci. Technol. 37, 798–804.

Jeannottat, S., Hunkeler, D., 2012. Chlorine and carbon isotopes fractionation during volatilization and diffusive transport of trichloroethene in the unsaturated zone. Environ. Sci. Technol. 46, 3169–3176.

Kuder, T., Wilson, J.T., Kaiser, P., Kolhatkar, R., Philp, P., Allen, J., 2005. Enrichment of stable carbon and hydrogen isotopes during anaerobic biodegradation of MTBE: microcosm and field evidence. Environ. Sci. Technol. 39, 213–220.

Kuder, T., Philp, P., Allen, J., 2009a. Effects of volatilization on carbon and hydrogen isotope ratios of MTBE. Environ. Sci. Technol. 43, 1763–1768.

Kuder, T., Philp, P., Allen, J., 2009b. Effect of volatilization on carbon and hydeogen isotope ratios of MTBE. Environ. Sci. Technol. 43, 1763–1768.

Ladji, R., Yassaa, N., Balducci, C., Cecinato, A., Meklati, B.Y., 2009. Annual variation of particulate organic compounds in PM_{10} in the urban atmosphere of Algiers. Atmos. Res. 92, 258–269.

Li, J.J., Wang, G.H., Zhou, B.H., Cheng, C.L., Cao, J.J., Shen, Z.X., An, Z.S., 2012. Airborne particulate organics at the summit (2060 m, a.s.l.) of Mt. Hua in central China during winter: implications for biofuel and coal combustion. Atmos. Res. 106, 108–119.

Lin, J., 2004. Characterization of n-alkanes in urban submicron aerosol particles (PM_1). Atmos. Environ. 38, 2983–2991.

Ma, S.X., Peng, P.A., Song, J.Z., Zhao, J.P., He, L.L., Sheng, G.Y., Fu, J.M., 2010. Stable carbon isotopic compositions of organic acids in total suspended particles and dusts from Guangzhou, China. Atmos. Res. 98, 176–182.

Mancini, S.A., Lacrampe-Couloume, G., Jonker, H., Breukelen, B.M.V., Groen, J., Volkering, F., Lollar, B.S., 2002. Hydrogen isotopic enrichment: an indicator of biodegradation at a petroleum hydrocarbon contaminated field site. Environ. Sci. Technol. 36, 2464–2470.

Mansuy, L., Philp, R.P., Allen, J., 1997. Source identification of oil spills based on the isotopic composition of individual components in weathered oil samples. Environ. Sci. Technol. 31, 3417–3425.

Mariotti, A., Germon, J.C., Hubert, P., Kaiser, P., Letolle, R., Tardieux, A., Tardieux, P., 1981. Experimental determination of nitrogen kinetic isotope fractionation: some principles; illustration for the denitrification and nitrification processes. Plant Soil 62, 413–430.

Meckenstock, R.U., Morasch, B., Warthmann, R., Schink, B., Annweiler, E., Michaelis, W., Richnow, A.H.H., 1999. $^{13}C/^{12}C$ isotope fractionation of aromatic hydrocarbons during microbial degradation. Environ. Microbiol. 1, 409–414.

Oba, Y., Naraoka, H., 2007. Carbon and hydrogen isotope fractionation of acetic acid during degradation by ultraviolet light. Geochem. J. 41, 103–110.

Oba, Y., Naraoka, H., 2008. Carbon and hydrogen isotopic fractionation of low molecular weight organic compounds during ultraviolet degradation. Org. Geochem. 39, 501–509.

O'Malley, V.P., Abrajano, T.A.J., Hellou, J., 1994. Determination of the $^{13}C/^{12}C$ rations of individual PAH from environmental samples: can PAH sources be apportioned? Org. Geochem. 21, 809–822.

Pond, K.L., Huang, Y.S., Wang, Y., Kulpa, C.F., 2002. Hydrogen isotopic composition of individual *n*-alkanes as an intrinsic tracer for bioremediation and source identification of petroleum contamination. Environ. Sci. Technol. 36, 724–728.

Poulson, S.R., Drever, J.I., 1999. Stable isotope (C, Cl, and H) fractionation during vaporization of trichloroethylene. Environ. Sci. Technol. 33, 3689–3694.

Rayleigh, L., 1902. LIX. On the distillation of binary mixtures. Philos. Mag. Ser. 6 (4), 521–537.

Richnow, H.H., Eschenbach, A., Mahro, B., Stner, M.K., Annweiler, E., Seifert, R., Michaelis, W., 1999. Formation of nonextractable soil residues: a stable isotope approach. Environ. Sci. Technol. 33, 3761–3767.

Richnow, H.H., Annweiler, E., Michaelis, W., Meckenstock, R.U., 2003. Microbial in situ degradation of aromatic hydrocarbons in a contaminated aquifer monitored by carbon isotope fractionation. J. Contam. Hydrol. 65, 101–120.

Sun, Y.G., Chen, Z.Y., Xu, S.P., Cai, P.X., 2005. Stable carbon and hydrogen isotopic fractionation of individual *n*-alkanes accompanying biodegradation: evidence from a group of progressively biodegraded oils. Org. Geochem. 36, 225–238.

Ulevicius, V., Byčenkienė, S., Remeikis, V., Garbaras, A., Kecorius, S., Andriejauskienė, J., Jasinevičienė, D., Mocnik, G., 2010. Characterization of pollution events in the East Baltic region affected by regional biomass fire emissions. Atmos. Res. 98, 190–200.

Wang, Y., Huang, Y.S., 2001. Hydrogen isotope fractionation of low molecular weight *n*-alkanes during progressive vaporization. Org. Geochem. 32, 991–998.

Wang, Y., Huang, Y.S., 2003. Hydrogen isotopic fractionation of petroleum hydrocarbons during vaporization: implications for assessing artificial and natural remediation of petroleum contamination. Appl. Geochem. 18, 1641–1651.

Xie, M.J., Wang, G.H., Hu, S.Y., Han, Q.Y., Xu, Y.J., Gao, Z.C., 2009. Aliphatic alkanes and polycyclic aromatic hydrocarbons in atmospheric PM_{10} aerosols from Baoji, China: implications for coal burning. Atmos. Res. 93, 840–848.

Yamamoto, S., Kawamura, K., 2010. Compound-specific stable carbon and hydrogen isotopic compositions of *n*-alkanes in urban atmospheric aerosols from Tokyo. Geochem. J. 44, 419–436.

Yamamoto, S., Kawamura, K., 2011. Stable hydrogen isotope ratios of *n*-alkanes in atmospheric aerosols from Okinawa. Jpn. Res. Org. Geochem. 27, 81–89.

Yamamoto, S., Kawamura, K., 2012. Application of urea adduction technique to polluted urban aerosols for the determination of hydrogen isotopic composition of *n*-alkanes. Int. J. Environ. Anal. Chem. 92, 302–312.

Young, L.H., Wang, C.S., 2002. Characterization of *n*-alkanes in $PM_{2.5}$ of the Taipei aerosol. Atmos. Environ. 36, 477–482.

Zhou, J.B., Wang, T.G., Zhang, Y.P., Zhong, N.N., Medeiros, P.M., Simoneit, B.R.T., 2009. Composition and sources of organic matter in atmospheric PM_{10} over a two year period in Beijing, China. Atmos. Res. 93, 849–861.

Zwank, L., Berg, M., Elsner, M., Schmidt, T.C., Schwarzenbach, R.P., Haderlein, S.B., 2005. New evaluation scheme for two-dimensional isotope analysis to decipher biodegradation processes: application to groundwater contamination by MTBE. Environ. Sci. Technol. 39, 1018–1029.